

## Supporting Information

### Material synthesis:

The ZnO-CdSe nano support was first synthesized by a sequential growth of CdSe and ZnO as we previously reported.<sup>1</sup> CdSe particles were obtained through the reaction of Na<sub>2</sub>SeSO<sub>3</sub> and Cd(NO<sub>3</sub>)<sub>2</sub>. The Na<sub>2</sub>SeSO<sub>3</sub> aqueous solution was prepared by refluxing Se powder in an aqueous Na<sub>2</sub>SO<sub>3</sub> solution at 80 °C overnight. 0.64 g Cd(NO<sub>3</sub>)<sub>2</sub> and 14.70 g sodium citrate were dissolved into 100 mL water to form a solution which was then mixed with freshly prepared 0.1 M Na<sub>2</sub>SeSO<sub>3</sub> (100 mL) into a flask and heated in water bath at 60 °C for 15 minutes. The red precipitate was collected by centrifugation at 5000 rpm for 10 minutes and extensively washed, after which the supernatant was decanted and discarded. The growth of ZnO nano-rod was then carried out by Zeng's method.<sup>2</sup> 1.487 g zinc nitrate [Zn(NO<sub>3</sub>)<sub>2</sub> · 6H<sub>2</sub>O] and 6.000 g NaOH were dissolved in 10 mL deionized water (the molar ratio of Zn<sup>2+</sup> to OH<sup>-</sup> was 1:30). Some CdSe particles produced previously were dispersed into 100 mL ethanol which was added to the solution containing Zn precursor. 5 mL ethylenediamine (EDA) was also put into the mixture, which was then transferred to a 250 mL covered plastic container. This was kept at room temperature under constant stirring until the red mixture turned white. The white crystalline product was then collected by centrifuge and was washed with deionized water and pure ethanol. The final product was dried in an oven at 60 °C for 12 h. The loading of 5 wt% Pd onto above synthesized support was achieved by the impregnation method; the ZnO-CdSe nano support was immersed into a Pd(NO<sub>3</sub>)<sub>2</sub> ethanol solution and the mixture was kept stirring at 50 °C until the ethanol solvent was evaporated. The harvested powder was calcined at 400 °C for 2h. The Pd@Zn

core-shell structure was obtained through the H<sub>2</sub> pre-treatment at 250°C for 1 h.

### **Characterization Techniques:**

#### **Inductive coupled plasma – atomic emission spectrometry (ICP-AES)**

ICP-AES was performed to determine the concentration of CdSe in the ZnO-CdSe supports and the data was collected on an IRIS Intrepid II XSP spectrometer. The obtained values are displayed in the related figures.

#### **X-ray diffraction (XRD)**

The data was collected using a Philips PW1729 diffractometer, operating in Bragg-Brentano focusing geometry and using CuK $\alpha$  radiation ( $\lambda = 1.5418 \text{ \AA}$ ) from a generator operating at 40 kV and 30 mA.

#### **Diffusion reflectance spectroscopy (DRS)**

DRS was employed to determine the band structure of the catalyst and the data was collected on a Perkin Elmer Lambda 750S Uv/vis spectrometer.

#### **Time resolved photoluminescence (PL) spectra**

To probe dynamics and in particular lifetimes of the electrons and holes, time-resolved photoluminescence (TRPL) measurement has been conducted on sample 1 (0.0 wt% CdSe) and sample 4 (26.4 wt% CdSe). The data were collected on a commercial Ti: Sapphire regenerative amplifier laser system (800 nm, 40 fs, 1 kHz, 3.5 mJ/ pulse) and home built spectrometers.

For the TRPL, the 300 nm excitation pulse was generated by the optical parametric amplifiers (OPA) and the measurements were done with samples in the solid state. The signals were collected by a spectrograph and detected with a liquid nitrogen cooled CCD detector. All the measurements were conducted at room temperature and atmospheric pressure.

#### **X-ray photoelectron spectroscopy (XPS)**

XPS was performed using Kratos Ltd XSAM800.

#### **Energy-dispersive X-ray spectroscopy (EDX) and Transmission electron**

### **microscopy (TEM)**

EDX and high resolution TEM images were obtained on an Analytical FEI Tecnai 30 electron microscope operated at an acceleration voltage of 300 kV. The samples were prepared by placing a drop of nanoparticle ethanol suspension onto a carbon-coated copper grid, and allowing the solvent to evaporate.

### **Chemisorption of CO**

The chemisorption uptake of CO was measured to determine the number of Pd active site per gram catalyst with the ratio of Pd: CO= 1. The samples were measured on a Micromeritics ASAP 2020 (M+C) analyzer. The samples with variable concentration of CdSe (samples 1-4) were pre-reduced at 523 K and evacuated for 1 h at 523 K to ensure a high surface cleanness. An initial isotherm was measured in an adsorbate pressure range of 100-600 Torr at a precisely controlled temperature of 308 K. Subsequently evacuation at 308 K for 30 min was conducted to remove the weak reversibly adsorbed CO molecules before measuring another repetitive isotherm under the same conditions as the initial one. The difference between the repetitive and the initial isotherm is denoted as the uptake of irreversibly chemisorbed CO on catalysts.

### **Characterization results:**

#### **TRPL for the CdSe-ZnO supports:**

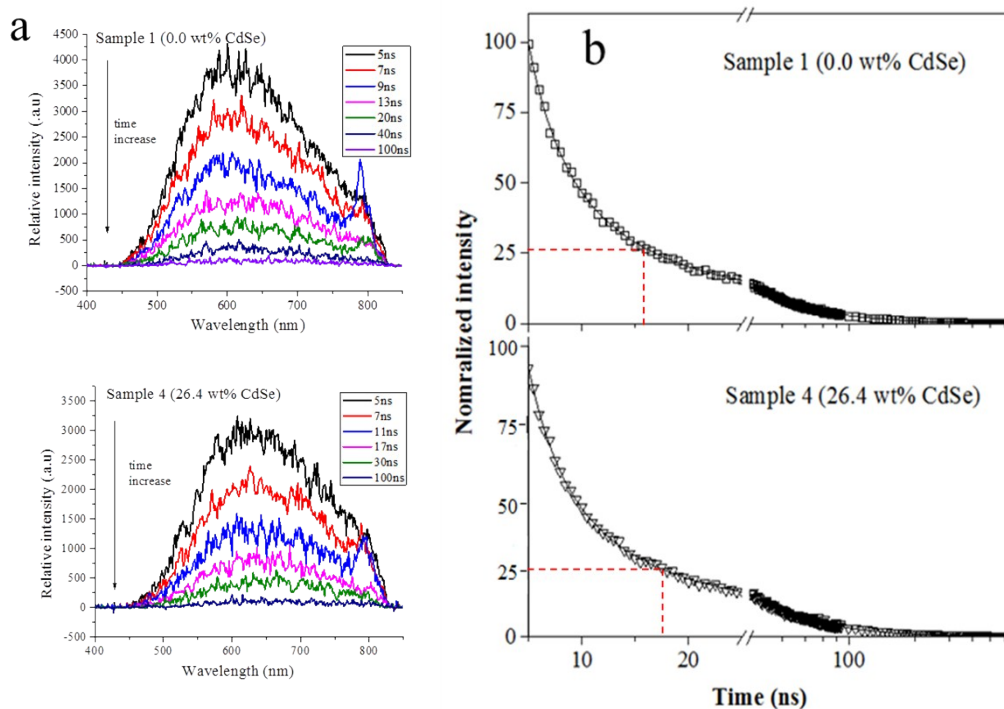


**Fig. S1.** (a) Time-resolved emission spectra of sample 1(0.0 wt% CdSe) and sample 4 (26.4 wt% CdSe) before reduction in the solid state at delay times within hundreds nanoseconds after excitation at 300 nm; (b) Experimental and fitted (solid lines) kinetic decay profiles obtained from integrated intensity of the time-resolved emission spectra of sample 1 (0.0 wt% CdSe) and sample 4 (26.4 wt% CdSe).

### XPS and TEM for the reduced Pd/ CdSe-ZnO samples

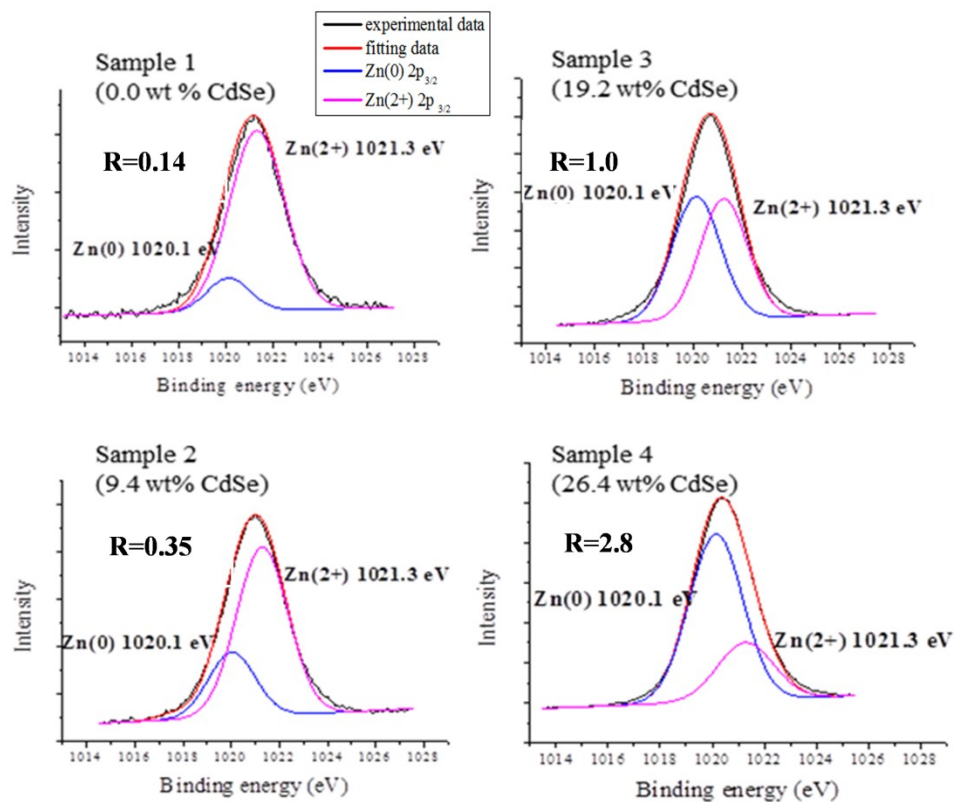


**Fig. S2-1.** The XPS curves of Zn in samples 1-4 after reduction in H<sub>2</sub> at 250°C and the corresponding fittings into Zn (2+) and Zn (0). (R represents the signal ratio of Zn(0): Zn(2+))

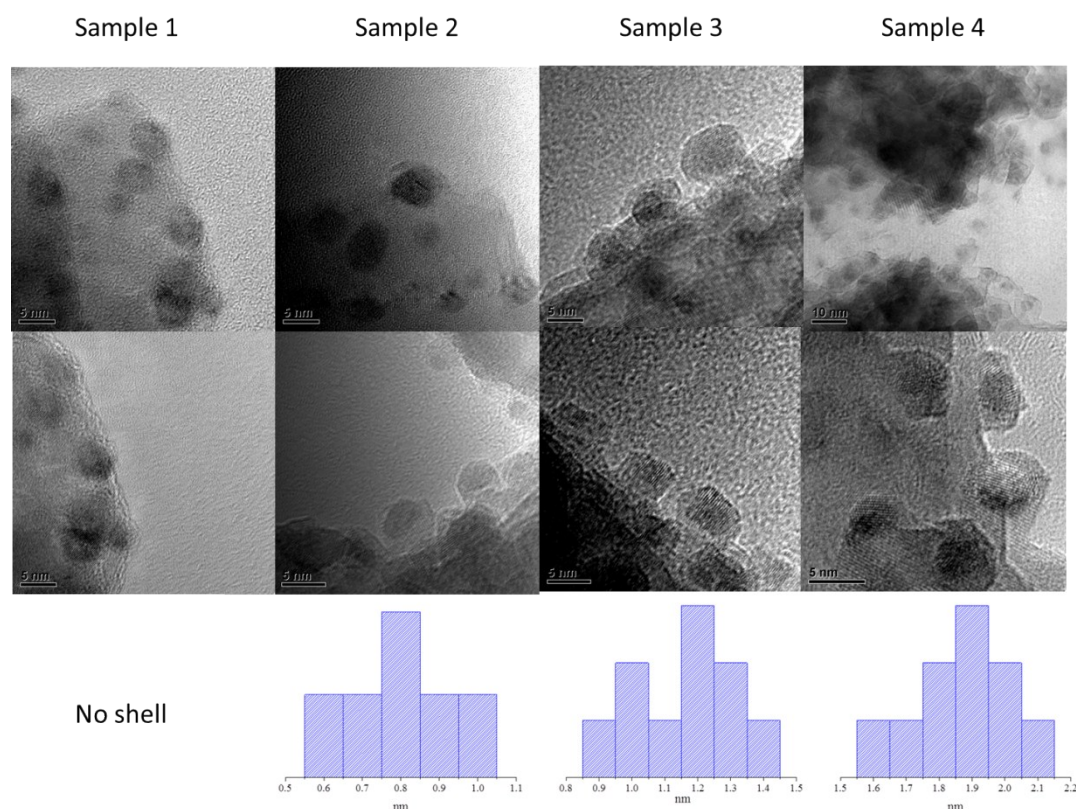


**Fig. S2-2.** The TEM images of Pd@Zn nano-particles in reduced samples 1-4 and the corresponding thickness distributions of Zn shells.

### Catalytic test of CO<sub>2</sub> hydrogenation:

Catalyst tests in hydrogenation of CO<sub>2</sub> were carried out in a tubular fixed bed reactor (12.7 mm outside diameter) by using a catalyst weight of 0.1 g. CO<sub>2</sub>/H<sub>2</sub> reaction mixture with molar ratio of 1:2.8 was fed at a rate of 30 stp mL min<sup>-1</sup> (stp = standard temperature and pressure; P = 101.3 kPa, T = 298 K) through the catalyst bed. Before each test, the catalyst was pre-reduced at 280 °C for 2 h under the H<sub>2</sub> flow (20 stp mL min<sup>-1</sup>). The products were analysed by a gas chromatograph equipped with a thermal conductivity detector (TCD). All the samples were tested at least twice to confirm the reproducibility.

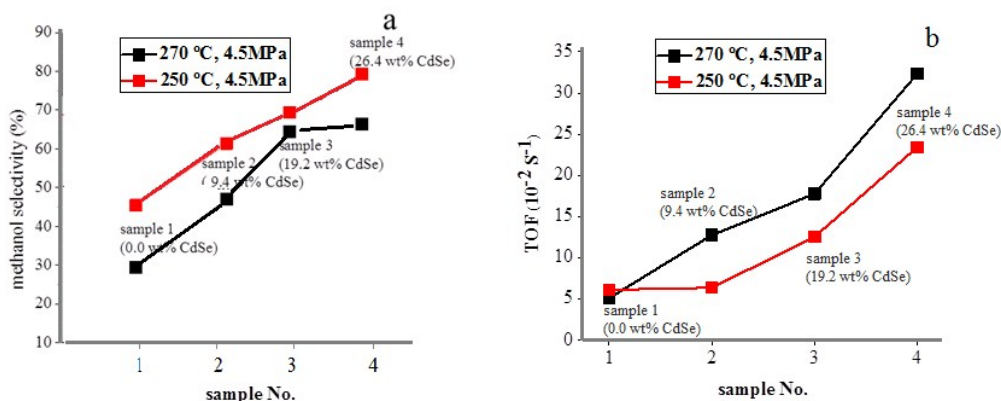


**Fig. S3.** The methanol selectivities and TOF values of samples 1-4 at 270 °C (black) and 250 °C (red), 4.5 MPa.

## DFT calculations

### Calculation method

PBE functional was used to do the spin-polarized DFT calculations by using the Vienna ab initio Simulation Package (VASP).<sup>3</sup> The project-augmented wave (PAW)<sup>4</sup> method was used to describe the interaction between atomic cores and electrons. Wave functions were expanded in plane waves with an energy cutoff of 400 eV. For integrations over the Brillouin zone, we used a  $5 \times 5 \times 1$  Monkhorst-Pack grid for all calculations. The structure optimizations were converged until the Hellman-Feynman force on each ion was less than  $0.02 \text{ eV}/\text{\AA}$ . The calculated lattice parameter of bulk Pd was  $3.95 \text{ \AA}$ , which is in good agreement with the values reported from previous studies.<sup>5, 6</sup>

The Pd (111)-based surfaces were modeled by 4-layer slabs repeated in a  $4 \times 4$  surface unit cell with the bottom one layer being fixed to the bulk parameters, while other layers were allowed to fully relax. To avoid interactions between slabs, all slabs were separated by a vacuum gap greater than  $10 \text{ \AA}$ . Previous experimental studies<sup>7, 8</sup> suggested that the Zn atoms are contained entirely and distributed uniformly in the topmost layer of Pd (111) substrate after annealing when the Zn coverage is under 0.5 monolayer (ML). For coverage around 0.5 ML, the  $p(2 \times 1)$  PdZn (1:1) surface alloy is formed. Further increasing the Zn coverage will not break the  $(2 \times 1)$  phase. Instead, Zn will infiltrate into the sub-surface layer first and then to the deeper layers.

Accordingly, we constructed a p(2×2) 1ML-PdZn (3:1) surface alloy deposited Pd (111) (case B in Scheme 1) to represent the case of Zn coverage of  $\sim 0.25$  ML. A p(2×1) 1ML-PdZn (1:1) surface alloy deposited Pd (111) (case C in Scheme 1) was then used to represent the case of Zn coverage  $\sim 0.5$  ML. To describe the case of highest Zn coverage ( $\sim 1$  ML), a p(2×1) 2ML-PdZn (1:1) surface alloy deposited Pd (111) (case D in Scheme 1), which was regarded to be more stable than the case C,<sup>9</sup> was constructed.

The binding energy (BE) of an adsorbate to the substrate was calculated as follows:

$$BE = E_{ad} + E_{sub} - E_{ad/sub},$$

where  $E_{ad}$ ,  $E_{sub}$  and  $E_{ad/sub}$  are the DFT total energies of gas-phase adsorbate, clean substrate and adsorption complex, respectively.

Transition states were located by using the climbing-image nudged elastic band (CI-NEB) method.<sup>10, 11, 12</sup>

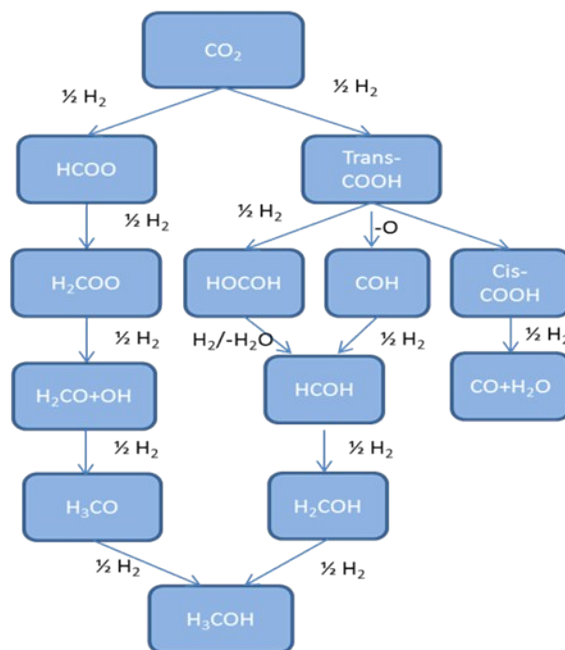


**Fig. S4.** The reported possible pathways in CO<sub>2</sub> hydrogenation,<sup>13,14</sup>

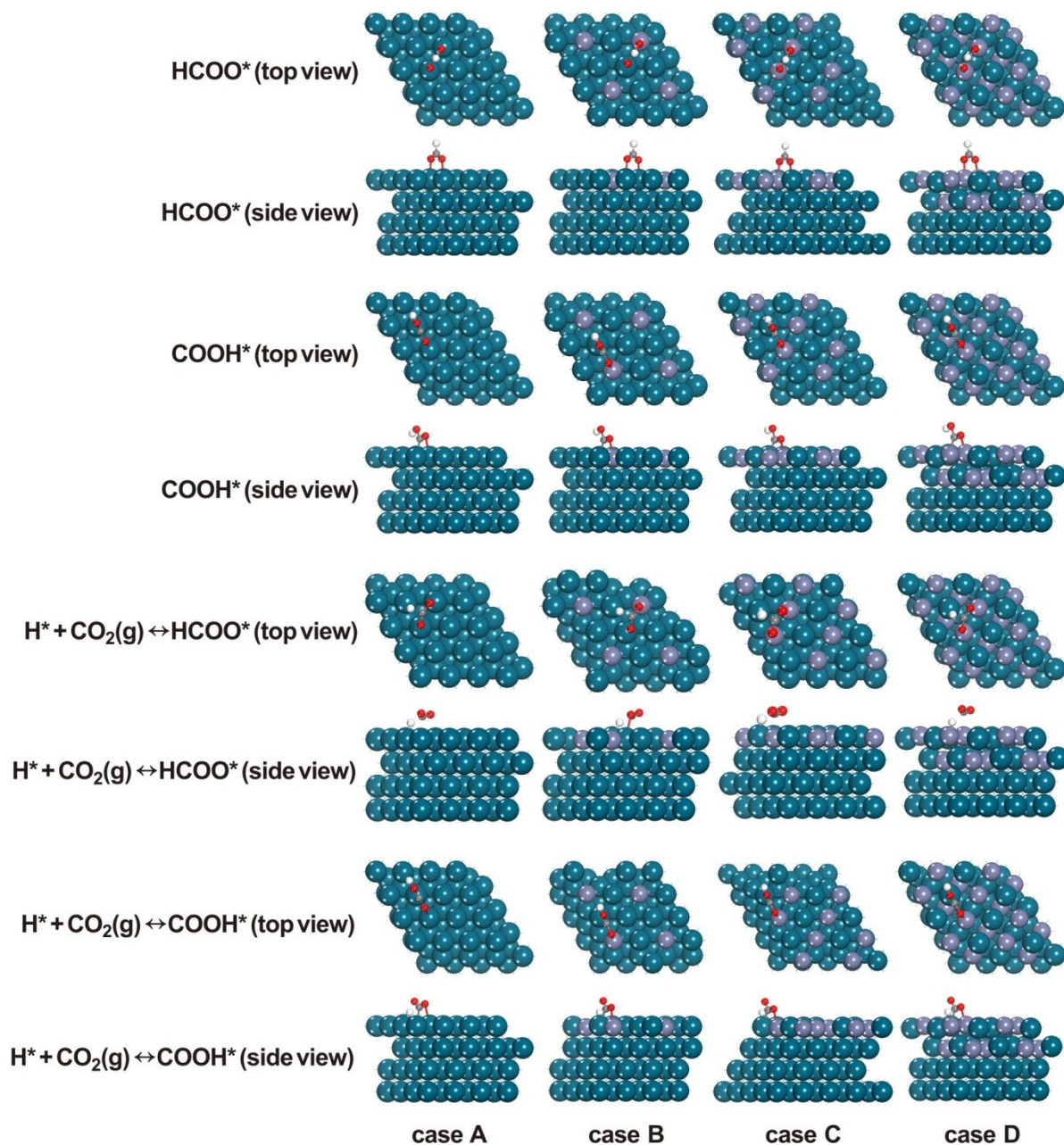


**Fig. S5.** Corresponding structures of the species in CO<sub>2</sub> hydrogenation to HCOO\* and COOH\* at cases A-D, Pd, Zn, H, C and O atoms are in cyan, purple, white, grey and red, respectively..

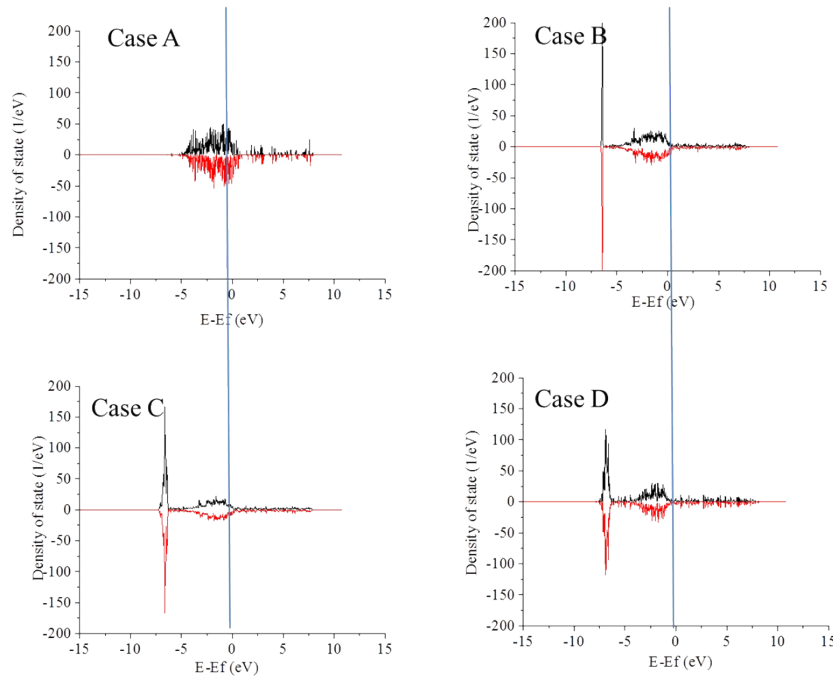


**Fig. S6.** The calculated density of states (DOS) for the surface atoms of Pd cases A-D.

**Table S1** The calculated d-band center for the cases A-D

Cases	A	B	C	D
d-band center (eV)	-1.40	-2.63	-3.92	-4.19

The density of states diagrams for Pd cases A→D are shown in Fig. S6. It is obvious that a localized narrow band at low energies is observed to replace the states at Fermi-edge which is indicative of the strong Pd-Zn covalent bonds. Due to the growth of this low position band with the increasing Zn content, the calculated d band center position downshifts progressively from case A to D as -1.40 eV, -2.63 eV, -3.92 eV, -4.19 eV. The difference in electronegativity between Zn (1.65) and Pd (2.2) implies that the Pd atoms in PdZn should get negative charge from neighbour Zn atoms through the bonding interaction of Pd and Zn. As shown in Fig. 5 (main manuscript), the d band filling of PdZn rises with increasing content of Zn, which confirms the charge transfer from Zn to Pd.

References:

- 1 F. Liao, Z. Zeng, C. Eley, Q. Lu, X. Hong, S. C. E. Tsang, *Angew. Chem. Int. Ed. (VIP)*. 2012, **51**, 5832-5836.
- 2 B. Liu, & H. C. Zeng, *Langmuir*, **2004**, 20, 4196–4204.
- 3 G. Kresse, & J. Hafner, *Phys. Rev. B* 1994, **49**, 14251–14269.
- 4 P. E. Blöchl, *Phys. Rev. B* 1994, **50**, 17953–17979.
- 5 A. A. B. Padama, & H. Kasai, *J. Chem. Phys.* 2014, **140**, 244707.
- 6 R. S. Johnson, *et al. Phys. Chem. Chem. Phys.* 2013, **15**, 7768–7776 .
- 7 J. M. MacLeod, J. A. Lipton-Duffin, A. Baraldi, R. Rosei, & F. Rosei, *Phys. Chem. Chem. Phys.* 2013, **15**, 12488–12494.
- 8 J. A. Lipton-Duffin, *et al. Phys. Chem. Chem. Phys.* 2014, **16**, 4764–4770.
- 9 G. Mills, & H. Jónsson, *Phys. Rev. Lett.* 1994, **72**, 1124–1127.
- 10 G. Mills, H. Jónsson, & G. Schenter, *Surf. Sci.* 1995, **324**, 305–337.
- 11 G. Henkelman, & H. Jónsson, *J. Chem. Phys.* 2000, **113**, 9978–9985.
- 12 G. Henkelman, B. P. Uberuaga, & H. Jónsson, *J. Chem. Phys.* **113**, 2000, 9901–9904.
- 13 Y.-F. Zhao *et al. J. Catal.* 2011, **281**, 199–211.
- 14 M. Y. Clarence, *et al. Catal Lett.* 2009, **128**, 221–226.